Communication in Physical Sciences 2019, 4(2): 118-132 https://journalcps.com/

Joint Effect of Ethanol Extract of Orange Peel and halides on the Inhibition of the Corrosion of Aluminum in 0.1 M HCl: An approach to Resource Recovery

Richard Alexis Ukpe
Received 08 November 2019/Accepted 12 November 2019/Published online: 30 December 2019

Abstract *Resource recovery is the science of creating valuable products from waste. Successful resource recovery can reduce the burden of waste disposal. In this study, attempt is made to utilized ethanol extract of orange peel waste as a corrosion inhibitor for mild steel in solution of HCl. Ethanol extract behaved as adsorption inhibitor and the ranged obtained for the inhibition efficiencies of various concentrations of the extract were Calculated inhibition efficiency ranged from 35.03 to 60.08 %, 30.02 to 52.61%, 28.04 to 46.44 % and from 25.98 to 43.34 %. However, in the presence of KBr, KI and KCl, the enhanced range were 40.95 to 71. 02, 40.62 to 71.07 and from 84.22 to 88.12 %. Calculated synergistic parameters were greater than unity indicating that the adsorption of ethanol extract of orange peel waste was enhance by synergistic interaction with halides. Statistical analysis of variance indicated that temperature and concentration have statistical weight of contributing to the inhibition efficiency of the extract. The prevalence of physical adsorption mechanism was confirmed through free energy of adsorption deduced from the fitted adsorption isotherms including Langmuir, Freundlich, Temkin, El Awardy et al and Dubinin-Radushkevich isotherms. However, joint adsorption of ethanol extract of orange peel waste did not obey the Temkin and Freundlich isotherm except the Langmuir isotherm, which displayed plots with negative slope (a reversal of what were obtained in the absence of the halides). FTIR of the extract indicated the presence of functional groups that are liken to those that are known good corrosion inhibitors.*

Key Words: *Resource recovery, orange peel waste, corrosion inhibitor, aluminum*

Richard Alexis Ukpe
Federal University, Otuoke, Bayelsa State, Nigeria
Email: ukpera@fuotuoke.edu.ng
Orcid id: 0000-0002-1010-4933

1.0 Introduction

Development of corrosion inhibitors is necessary in order to protect metals against degradation through electrochemical and environmental attacks (Ogoko *et al*., 2009). It has been established that among all the options available for preventing metals (in industrial installations) against degradation, the use of inhibitors is one of the best (Ye *et al.,* 2019). Practically, corrosion inhibitors are derived or synthesized and the essential requirements are possession of heteroatom (to facilitate adsorption), aromaticity, suitable functional groups and conjugated or π-electron bond ((Eddy and Awe, 2018). Several organic and inorganic compounds have met these conditions but recently, additional concerns are centered on the environmental requirements which is aimed at replacing toxic and expensive corrosion inhibitors with their green counterparts (Eddy, 2010). According to Ebenso *et al*. (2008), green corrosion inhibitors are cheap, biodegradable, easily accessible and environmentally friendly. Most green corrosion inhibitors in use are products or extracts of plants and animals. Consequently, several green corrosion inhibitors have been reported for the corrosion of metals including *Piper guinensis* (Ebenso *et al.,* 2010), *Parinari polyandra*(Awe *et al., 2019) Lasianthera Africana* (Eddy *et al*., 2009a), *Piliostigma Thonningii* (Ameh and Eddy, 2018), *Aloe vera* (Eddy and Odoemelam, 2009), *Azadirachta indica* (Eddy and Mamza, 2009), *Phyllanthus amarus* (Eddy, 2009;Eddy and Awe, 2018), *Gongronema latifolium* (Eddy and Ebenso, 2010), *Gnetum Africana* (Eddy *et al*., 2009b), *Heinsia crinata* (Eddy and Odiongenyi, 2010), *Terminalia atappa* (Eddy *et al*., 2009c), *Hibiscus sabdariffa calyx* (Eddy *et al*., 2011a), *Occimium gratissimum* (Eddy *et al*., 2010a), *Solanum melongena (*Eddy *et al*., 2010b), *Andrographis leocapas gum (Eddy et al.,* 2011b), *Gloriosa superba* (Eddy *et al*., 2014) and others. Studies have

also been reported on the use of plant wastes as corrosion inhibitors for various metals. According to Ella *et* al. (2019), aqueous agrochemical waste significantly inhibited the corrosion of stainless steel in acidic media. Eddy *et* al. (2009) reported Musa species peel as excellent corrosion inhibitor for mild steel in acidic medium. Waste protein has also been found to be good corrosion inhibitor (Farag *et* al.,2018). Ismail *et* al., (2011) found that some plant wastes including Genus Musa, *Genus Saccharum* and *Citrullus Lanatus* wastes are good corrosion inhibitors for some metals in acidic medium. Mishurov *et al*., (2019) reported that plant biomass from vegetables were excellent corrosion inhibitors for steel in acidic medium. Stango and Vijayalasshmi (2018) reported the effect of orange peel on the inhibition of the corrosion of mild steel in 2 M HCl using weight loss, electrochemical impedance spectroscopy (EIS), potentiodynamic polarization and scanning electron microscopy (SEM) analysis. They obtained maximum inhibition efficiency of 99.19% for 0.25% of waste extract at room temperature. In our research group, we also found that mango peel waste is an excellent corrosion inhibitor for aluminium (Ukpen *et* al., 2014). To the knowledge of the author, there is no literature on the inhibition of aluminum corrosion by ethanol extract of orange peel, Therefore the present study is aimed at investigating the corrosion inhibition properties of ethanol, extract of orange peel in solution of HCl. According to Stango and Vijayalakshmi (2018), the chemical constituents of ethanol extract of orange peel is shown in the structures below. The structures compromise with the requirement listed for corrosion inhibitors, which prompted this study.

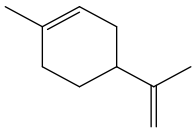

1-methyl-4-(prop-1-en-2-yl)cyclohex-1-ene

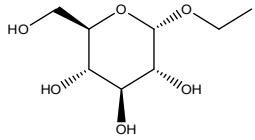

ethyl-alpha-d-glucopyranoside

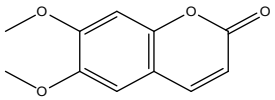

6,7-dimethoxy-2H-chromen-2-one

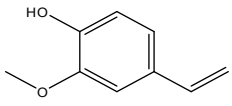

2-methoxy-4-vinylphenol

Chemical Structures of compounds in ethanol extract of Orange peel waste
(Source: Stango and Vijayalakshmi, 2018)

Potassium halides shall be used to enhance the corrosion inhibition of the extract, where they are weak. Also, FTIR spectrum of the extract shall be obtained in order to identify the functional groups in the Orange peel extract. .

2. 0 Materials and Methods

2. 1 Materials

Aluminium sheets of composition (wt %) Mn (0.6), P (0.36), C (0.15) and Si (0.03) were used for the study. The sheet was mechanically cut into coupons with dimension 5 x 4cm. The coupons were degreased by washing in absolute ethanol, dried in acetone and stored in moisture free desiccators before use (Agrawal *et al*., 2003; Jovancicervic *et al*., 1999).

Analar grade reagents were used. These included concentrated hydrochloric acid, ethanol and Al dust. Orange peel wastes (OPW) were gotten as domestic wastes from some homes in Ikot Ekpene. The waste materials were sun-dried, grounded into power sample and soaked in ethanol for one day. The soaked samples were respectively subjected to Soxhlet extraction and the ethanol extracts obtained for each sample were stored for used.

0.1 M HCl was prepared from stock solution of the acid and was stored in twenty four different containers. The first container was labelled as blank. Stock solution containing 0.1, 0.2, 0.3, 0.4 and 0.5 g of a given sample (per liter of the acid solution) were respectively prepared and preserved for use.

2. 2 Weight loss measurements

Previously weighed metal (aluminium sheet) was completely immersed in 250 ml of the test solution (different concentrations of acid, halides, or inhibitors) in an open beaker. The beaker was inserted into a water bath maintained at a temperature of 30 °C. Similar experiments were repeated at 40, 50 and 60 °C. In each case, the weight of the sample before immersion was measured using Scaltec high precision balance (Model SPB31) After every 24 hours, each sample was removed from the test solution, washed in a solution of NaOH containing aluminium dust and dried in acetone before re-weighing. The difference in weight for a period of 168 hours was taken as total weight loss. The inhibition efficiency (%η) for each inhibitor was calculated using the formula,

$$\%I = \left(1 - \frac{W_1}{W_2}\right) \times 100 \qquad (1)$$

where W_1 and W_2 are the weight loss (g) for aluminum in the presence and absence of the inhibitor. The degree of surface coverage θ is given by the equation 2

$$\theta = (1 - \frac{W_1}{W_2}) \quad (2)$$

The corrosion rates for aluminium corrosion in different concentrations of the acid was determined after 168 hours period of immersion and was calculated using equation 3

$$Corrosion\ rate\ (mpy) = \frac{534W}{DAT} \quad (3)$$

where W = weight loss (mg); D = density of specimen (g/cm^3), A = area of specimen (square inches) and T = period of immersion (hour).

2.3 Synergistic study

Synergistic study was carried out using weight loss. However, each concentration of the test solution was mixed with 0.06M of the respective halides (namely, KBr, KI and KCl), from the calculated inhibition efficiencies, synergistic parameters were calculated using the following equation,

$$S = \frac{1 - \eta_A + \eta_A\eta_B}{1 - \eta_{AB}} \quad (4)$$

2.4 Hydrogen evolution experiments

In thermometric experiment, the metal was inserted into a three-neck thermometric flask (which has provision for introducing thermometer, test solution and the metal). The system was properly lagged and changes in temperature were recorded every one minute. The reaction number and the inhibition efficiency were calculated using equations 4 and 5 respectively (Ameh and Eddy, 2018).

$$RN = \frac{T_t - T_0}{T_t} \quad (5)$$

$$\%\, I = \frac{\mathrm{RN}_{aq} - \mathrm{RN}_{wi}}{\mathrm{RN}_{aq}} \times \frac{100}{1} \quad (6)$$

where V_b is the volume of hydrogen gas evolved by the blank and V_t is the volume of H_2 evolved in the presence of the inhibitor, after time, t.

2.5 FTIR study

FTIR analysis of OPW was carried out using Scimadzu FTIR-8400S Fourier transform infra-red spectrophotometer. The sample was prepared in KBr and the analysis was carried out by scanning the sample through a wave number range of 400 to 4000 cm^{-1}.

3.0 Results and Discussion

3.1 Gravimetric and gasometric measurements

Figs. 1 to 4 show plots for the variation of weight loss with time for the corrosion of aluminum in 0.1 M HCl.

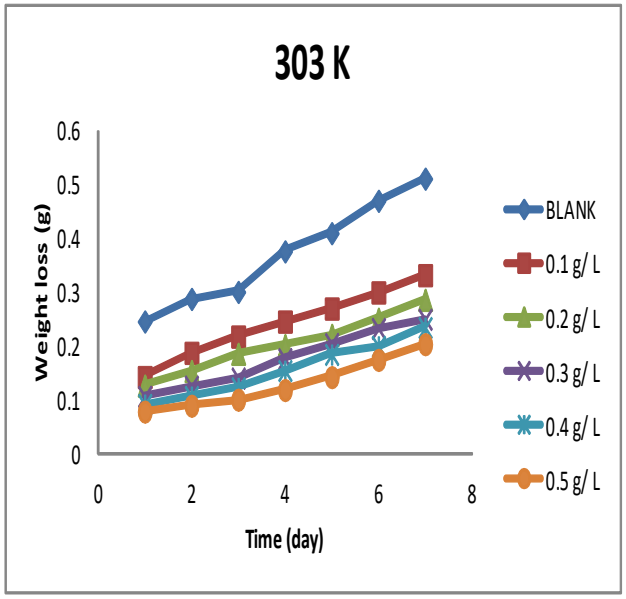

Fig. 1: Variation of weight loss with time for the corrosion of aluminium in 0.1 M HCl, containing various concentrations of orange peel (OPW) waste as an additive at 303 K

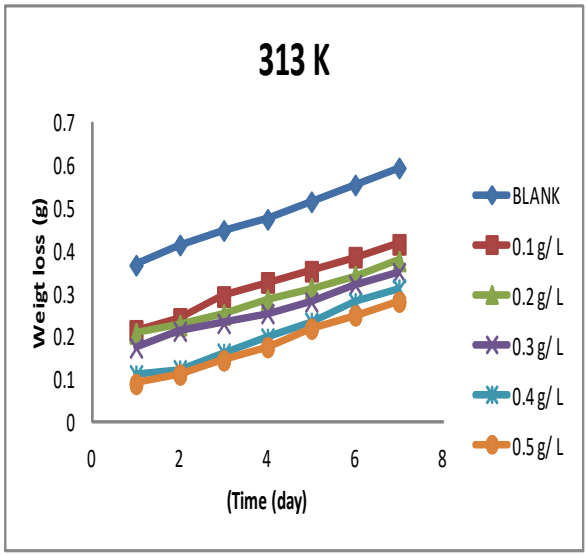

Fig. 2: Variation of weight loss with time for the corrosion of aluminium in 0.1 M HCl, containing various concentrations of orange peel (OPW) waste as an additive at 313 K

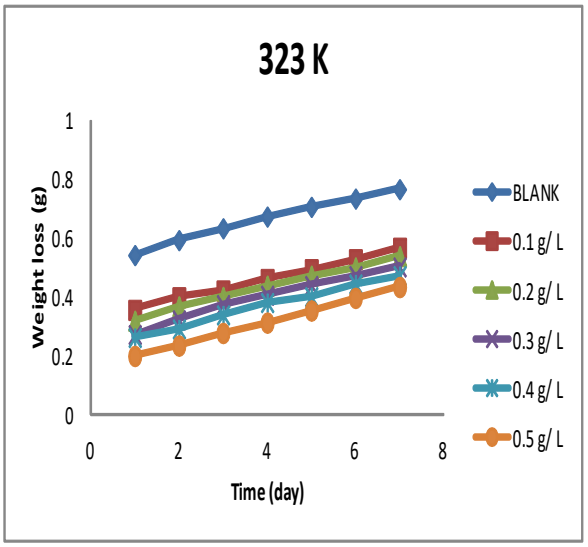

Fig. 3: Variation of weight loss with time for the corrosion of aluminium in 0.1 M HCl, containing various concentrations of orange peel (OPW) waste as an additive at 323 K

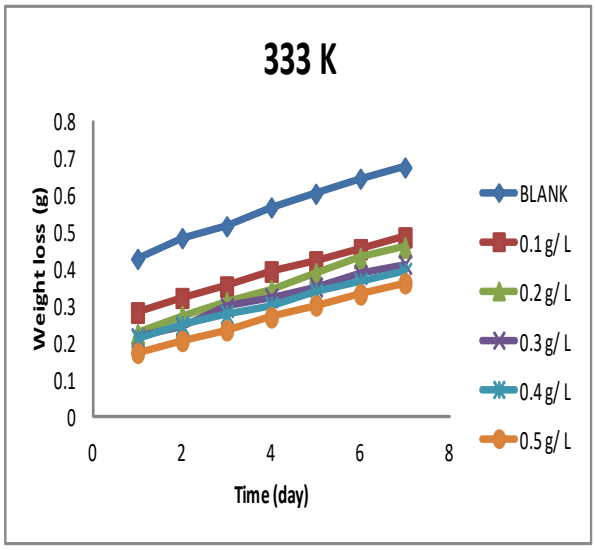

Fig. 4: Variation of weight loss with time for the corrosion of aluminium in 0.1 M HCl, containing various concentrations of orange peel (OPW) waste as an additive at 333 K

The plots reveal that weight loss of aluminum increases with increase in the period of contact and with increase in temperature. However, at all temperatures, weight loss of aluminum was found to decrease with increase in the concentration of ethanol extract of orange peel. Therefore, the extract retarded the rate of corrosion of aluminum in solution of HCl, indicating that ethanol extract of orange peel waste is an adsorption inhibitor for the corrosion of aluminum. The corrosion rate increases with temperature, which also explained while the inhibition efficiency decreases with temperature (Table 1). Adsorption inhibitor is an inhibitor whose inhibition efficiency increases with increase in concentration (Eddy *et al*., (2010). Also, the mechanism of adsorption can be deduced from the observed trend of variation of inhibition efficiency with temperature. Those whose inhibition efficiency increases with increase in temperature exhibit chemical adsorption while those whose inhibition efficiency decreases with temperature adopt physical adsorption mechanism. Therefore, ethanol extract of OPW is an adsorption inhibitor for aluminum in solution of HCl and the mechanism of its adsorption is physical adsorption.

Table 1: Corrosion rate (CR x 0.0001) of aluminium and inhibition efficiency of ethanol extract of orange peel in solutions of HCl at 303 to 333 K

C (g/L)	Corrosion rate				Inhibition efficiency			
	303K	**313K**	**323K**	**333K**	**303K**	**313K**	**323K**	**333K**
Blank	1.52	1.76	2.01	2.28	-	-	-	-
0.1	0.99	1.24	1.44	1.69	35.03	30.02	28.04	25.98
0.2	0.85	1.12	1.36	1.60	44.03	36.59	32.05	29.77
0.3	0.74	1.04	1.23	1.49	51.08	41.15	38.87	34.46
0.4	0.70	0.93	1.16	1.41	54.01	47.55	41.99	38.25
0.5	0.61	0.84	1.07	1.29	60.08	52.61	46.44	43.34

3.1.1 Statistical analysis

Analysis of variance aimed at investigating the effect of two treatments (temperature and concentration) on the corrosion inhibition efficiency of ethanol extract of OPW was carried out. The results obtained is presented in Table 2. From the

results obtained, it is evident that the calculated F value is higher than the critical F value (F_{crit}), for both temperature and concentration. Therefore, concentration and temperature contributed significantly to the inhibition efficiency of ethanol extract of OPW for aluminum

Table 2: Parameters obtained from analysis of variance (ANOVA) for effect of temperature and concentration on the inhibition efficiency of OPW

Source of Variation	*SS*	*df*	*MS*	*F*	*P-value*	*F crit*
Concentration	1066.94	4	266.73	109.45	2.46651E-09	3.25916673
Temperature	588.22	3	196.07	80.45	3.24259E-08	3.49029482
Error	29.25	12	2.44			
Total	1684.408	19				

3.1.2 Synergistic study

In the presence of 0.05 M of KI, KBr and KCl as additives, the inhibition efficiencies of various concentrations of ethanol extract of orange peel were enhanced as shown in Table 3. Significant enhancement in inhibition efficiencies of various concentrations of ethanol extract of orange peel waste (OPW) was observed, however, this observation does not translated to increase in adsorption except synergistic parameters are calculated. According to Eddy *et al*. (2009), synergistic parameter can be calculated using the following equation,

$$S = \frac{1 - I_A - I_B - I_A I_B}{1 - I_{AB}} \quad (7)$$

where I_A and I_B are inhibition efficiency of compound A and B respectively while I_{AB} is the inhibition efficiency of the combined compound. Calculated values of synergistic parameters for the various combinations of halides and OPW are also recorded in Table 3. Values of S are greater than unity indicating that the adsorption of OPW on aluminum surface is enhanced by KI, KCl and KBr. The synergistic parameters were highest for KCl and least for KI indicating that best efficiencies were obtained through synergistic combination of OPW with KCl, followed by KBr and by KI.

Table 3: Inhibition efficiencies of OPW, Joint OPW halides combinations and associated synergistic parameters

C	Inhibition efficiency (%I)				Synergistic parameter		
(g/L)	**KBr + OPW**	**KI + OPW**	**KCl + OPW**	**OPW**	**KBr +OPW**	**KI + OPW**	**KCl + OPW**
0.1	40.95	40.62	84.22	35.03	0.95	0.64	4.41
0.2	40.96	60.70	84..33	44.03	0.96	0.75	3.34
0.3	71.13	60.70	84.40	51.08	1.13	0.60	2.57
0.4	71.15	65.00	86.63	54.01	1.15	0.64	3.65
0.5	71.02	71.07	88.12	60.08	1.02	1.04	2.21

Inhibition efficiencies were also obtained from hydrogen evolution measurements. During corrosion, anodic dissolution of metal and cathodic evolution of hydrogen gas are constantly competing indicating that corrosion rate can be assessed by measuring the volume of hydrogen gas evolved at the cathode. This is the principle behind gasometric technique. Fig. 5 shows the variation of the volume of hydrogen gas evolved with time for the corrosion of aluminum containing various concentrations of ethanol extract OPW. Inhibition efficiencies of 0.1, 0.2, 0.3, 0.4 and 0.5 g/L of OPW were 66.22, 70. 33, 70.45, 74.33 and 77.45 % respectively.

3.2 Kinetic study

According to Eddy *et al.* (2011), corrosion reaction is a pseudo first order reaction that obeys the following equation (Ameh and Eddy, 2018),

$$-\log(weight\ loss) = \frac{k_1 t}{2.303} \quad (8)$$

where k_1 is the first order rate constant and t is the time. From the above, plotting of -log (weight loss) against time yielded straight lines at all temperatures

as shown in Figs. 6 to 9. The rate constant is related to the half-life of the metal in the acidic solution in the absence and presence of the inhibitor according to equation 9, (Ebenso *et al*., 2008))

$$t_{1/2} = \frac{0.693}{k_1} \quad (9)$$

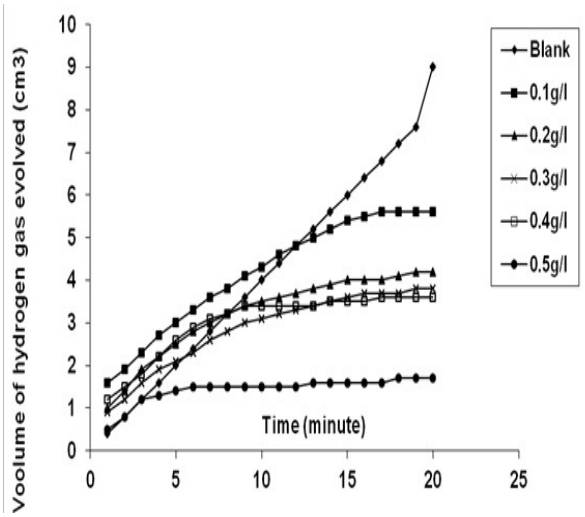

Fig. 5: Variation of volume of hydrogen gas evolved with time for the corrosion of aluminum in 0.1M HCl containing various concentrations of ethanol extract of OPW

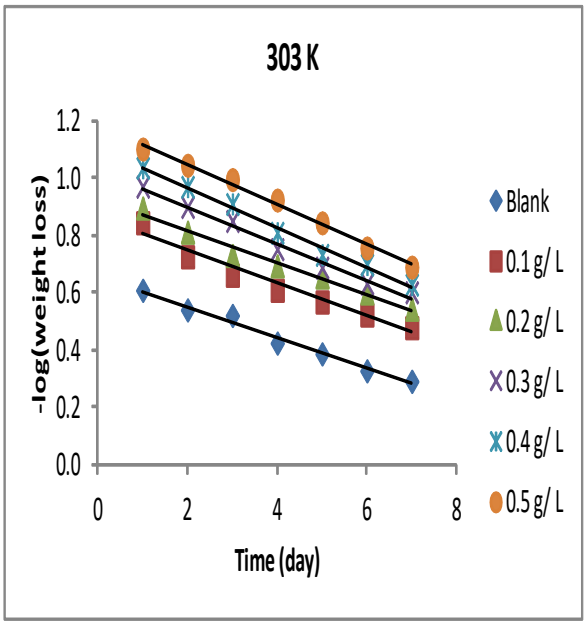

Fig. 6: Variation of –log(weight loss) with time for the corrosion of aluminium in 0.1 M HCl containing various concentrations of OPW at 303 K

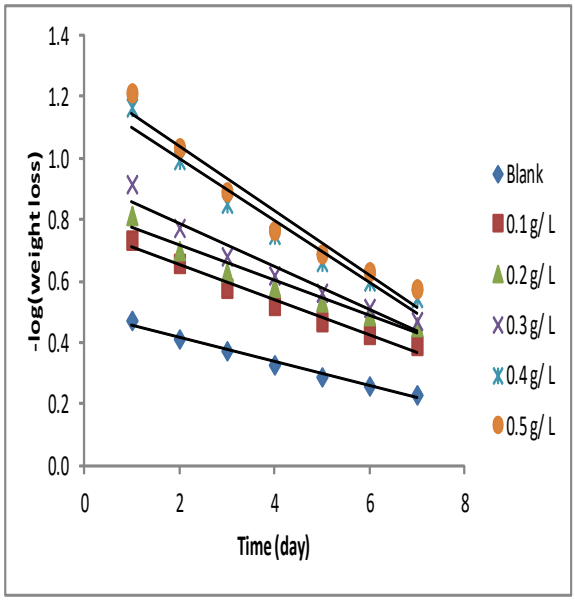

Fig. 7: Variation of –log(weight loss) with time for the corrosion of aluminium in 0.1 M HCl containing various concentrations of MPW at 313 K

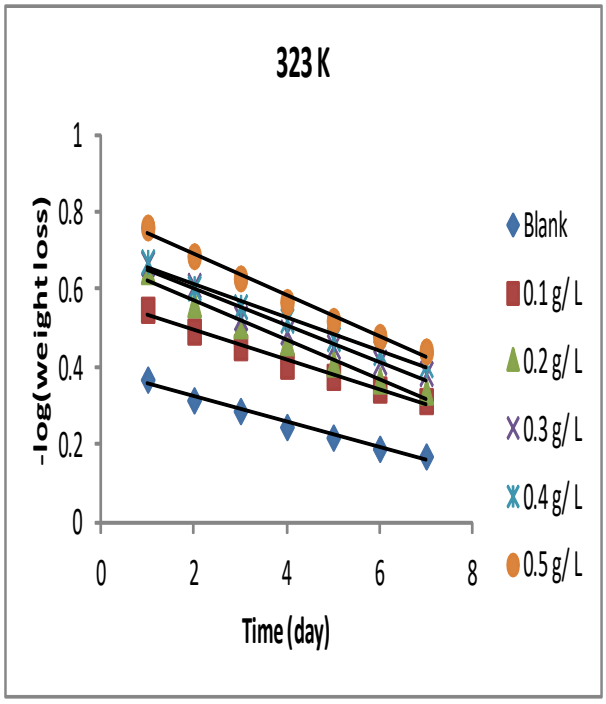

Fig. 8: Variation of –log(weight loss) with time for the corrosion of aluminium in 0.1 M HCl containing various concentrations of OPW at 323 K

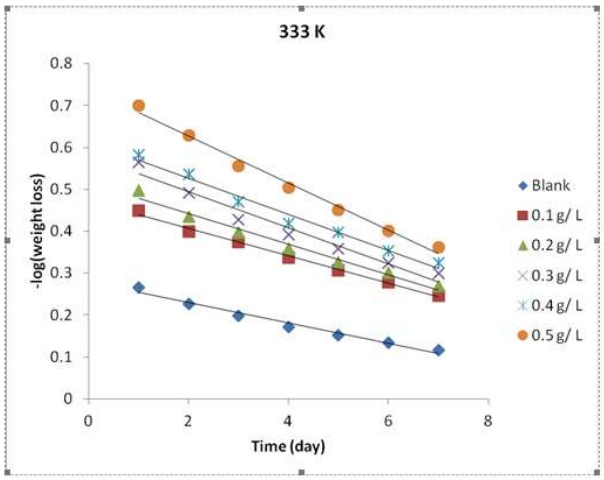

Fig. 9: Variation of –log(weight loss) with time for the corrosion of aluminium in 0.1 M HCl containing various concentrations of OPW at 333 K

3.3 Effect of temperature

The Arrhenius model is useful in calculating the minimum energy needed for the corrosion of aluminum to occur. The higher the energy, the better the inhibition process. The exponential and logarithm forms of the Arrhenius equations can be written according to equations 10 and 11 respectively (Eddy *et al.,* 2015)

$$CR = Aexp\left(\frac{-E_a}{RT}\right) \quad (10)$$

$$\ln(CR) = lnA - \frac{E_a}{RT} \quad (11)$$

Equation 11 is the functional form of the Arrhenius equation because a plot of the logarithm of the corrosion rate against the inverse of temperature gives slope and intercept equal to E_a/R and ln(A) respectively.

Table 3: Kinetic parameters for the inhibition of the corrosion of aluminium in 0.1 M HCl by OPW

System	Slope	K_1	$t_{1/2}$ (day)	R^2
Blank (0.1 M HCl)	0.0540	0.1244	2.0	0.9853
0.1 g/L OPW at 303 K	0.0570	0.1313	4.3	0.9601
0.2 g/L OPW at 303 K	0.0556	0.1280	4.7	0.9804
g/L OPW at 303 K	0.0644	0.1483	5.4	0.9859
0.4 g/L OPW at 303 K	0.0694	0.1598	5.3	0.9901
0.5 g/L OPW at 303 K	0.0702	0.1617	5.6	0.9924
Blank (0.1 M HCl)	0.0481	0.1108	2.1	0.9729
0.1 g/L OPW at 313 K	0.0337	0.0776	3.8	0.9916
0.2 g/L OPW at 313 K	0.0439	0.1011	6.2	0.9977
0.3 g/L OPW at 313 K	0.0485	0.1117	6.3	0.9862
0.4 g/L OPW at 313 K	0.0798	0.1838	6.9	0.9886
0.5 g/L OPW at 313 K	0.0850	0.1958	8.9	0.9855
Blank (0.1 M HCl)	0.0326	0.0751	5.7	0.9828
0.1 g/L OPW at 323 K	0.0387	0.0891	6.9	0.9867
0.2 g/L OPW at 323 K	0.0508	0.1170	6.4	0.9807
0.3 g/L OPW at 323 K	0.0473	0.1089	5.9	0.9714
0.4 g/L OPW at 323 K	0.0433	0.0997	7.8	0.9867
0.5 g/L OPW at 323 K	0.0530	0.1221	9.2	0.9876
Blank (0.1 M HCl)	0.0244	0.0562	5.4	0.9782
+0.1 g/L OPW at 333 K	0.0328	0.0755	7.0	0.9939
0.2 g/L OPW at 333 K	0.0364	0.0838	7.0	0.9814
0.3 g/L OPW at 333 K	0.0429	0.0988	8.3	0.9603
0.4 g/L OPW at 333 K	0.0432	0.0995	9.2	0.9798
0.5 g/L OPW at 333 K	0.0561	0.1292	12.3	0.9898

The Arrhenius plots for the corrosion of aluminum in 01 M HCl containing various concentrations of ethanol extract of OPW are presented in Fig. 10. Arrhenius parameters are recorded. Obedient of the corrosion data to the Arrhenius model was confirmed by excellent degree of fitness of the plots. Estimated values of the activation energies ranged from 14.62 to 20.85 J/mol. They were higher than the value of 11.22 J/mol obtained for the blank and tend to increase with increase in concentration. Therefore, the ease of adsorption of the inhibitor increases with its concentration.

3.4 Thermodynamic/adsorption consideration

Thermodynamic parameters are fundamental in predicting the feasibility and direction of the corrosion and the inhibition process. Eyring Transition state equation was applied to calculate the adsorption enthalpy and entropy changes. The equation can be written in the exponential form expressed by equation 12 (Ameh and Eddy, 2018),

$$CR = \frac{RT}{Nh} exp\left(\frac{\Delta S^0_{ads}}{T}\right) exp\left(\frac{-\Delta H^0_{ads}}{RT}\right) \qquad (12)$$

where N is the Avogadro's number, h is the Planck constant, R is the gas constant, ΔS^0_{ads} and ΔH^0_{ads} are standard entropy and enthalpy changes respectively. The logarithm of both sides of equation 12 (which gives equation 13) enables ΔS^0_{ads} and ΔH^0_{ads} to be estimated through the slope and intercept of the plots of $\ln\left(\frac{CR}{T}\right)$ versus 1/T respectively.

$$\ln\left(\frac{CR}{T}\right) = \ln\left(\frac{R}{Nh}\right) - \frac{\Delta S^0_{ads}}{T} + \frac{\Delta H^0_{ads}}{RT} \qquad (13)$$

The transition state plots for the corrosion of aluminum in the presence of various concentrations of OPW is shown in Fig. 11. Calculated thermodynamics parameters were also recorded in Table 4. The results indicated that the adsorption of OPW on aluminum surface is exothermic and occurs with increasing degree of orderliness (Eddy *et al*., 2011). Heat of adsorption and degree of orderliness increases with increase in concentration of OPW.

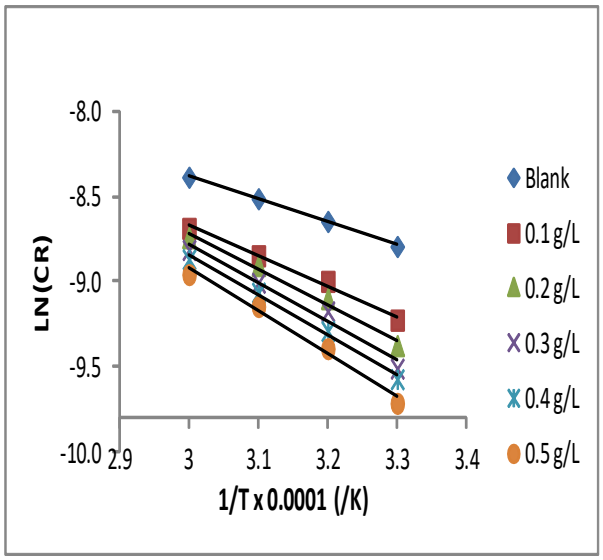

Fig. 10: Arrhenius plots for the inhibition of the corrosion of aluminium in solution of 0.1M HCl by OPW

Table 4: Arrhenius and thermodynamics parameters for the inhibition of the corrosion of aluminium by OPW

System	E_a (J/mol)	A	R^2	ΔH^0_{ads} (J/mol)	ΔS^0_{ads} (J/mol)	R^2
Blank	11.22	1.31E-05	0.9988	-8.60	-131.48	0.9983
0.1 g/L OPW	14.63	3.36E-05	0.9903	-12.02	-139.29	0.9863
0.2 g/L OPW	17.36	8.63E-05	0.9853	-14.74	-147.13	0.9803
0.3 g/L OPW	18.73	0.000131	0.9733	-16.10	-150.61	0.9650
0.4 g/L OPW	19.37	0.000156	0.9931	-16.76	-152.08	0.9912
0.5 g/L OPW	20.85	0.000247	0.9861	-18.24	-155.88	0.9824

Adsorption characteristics of a corrosion inhibitor can be predicted using adsorption isotherms. The general form of adsorption isotherm can be written as (Eddy *et al.,* 2012, 2018*)*

$$f(\theta, x)\exp(-2a\theta) = b_{ads}C \qquad (14)$$

where $f(\theta, x)$ is the configurational factor which depends upon the physical model and assumption underlying the derivative of the isotherm, θ is the surface coverage, C is the inhibitor concentration, x is the size ratio, 'a' is the molecular interaction parameter and b_{ads} is the equilibrium constant of adsorption process, In order to establish the best isotherms for the adsorption of OPW on aluminum surface, Data obtained from weight loss

measurements were used to test for the best isotherms that generated excellent degree of linearity Consequently, Temkin, Freundlich and El awardy isotherm best fitted the adsorption of OPW unto aluminum surface.

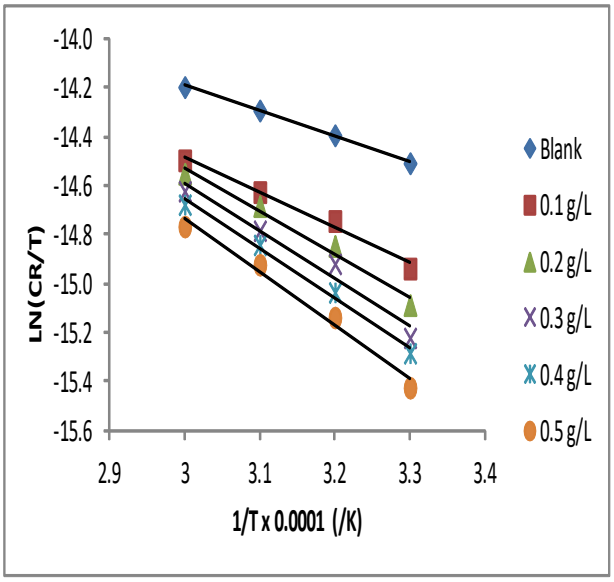

Fig. 11: Transition state plots for the inhibition of the corrosion of aluminium in solution of HCl by OPW

The assumptions of the Temkin adsorption model can be written according to equation 15 (Eddy *et al*., 2014)

$$\exp(-2a\theta) = b_{ads}C \quad (15)$$

The logarithm of both sides of equation 15 gives a linear model of the Temkin equation (equation 16)

$$\theta = \frac{-2.303}{2a} logb_{ads} - \frac{2.303}{2a} logC \quad (16)$$

Equation 16 indicates that a plot of θ versus logC should be linear with slope and intercept equal to $\frac{2.303}{2a}$ and $\frac{2.303}{2a}$ respectively. Fig. 12 shows Temkin isotherm for the adsorption of OPW on aluminium surface respectively. Adsorption parameters deduced from the plots are presented in Tables 5. The data reveal that high degrees of linearity were observed at all temperature and that the interaction parameters are positive, indicating the attractive behaviour of the inhibitors.

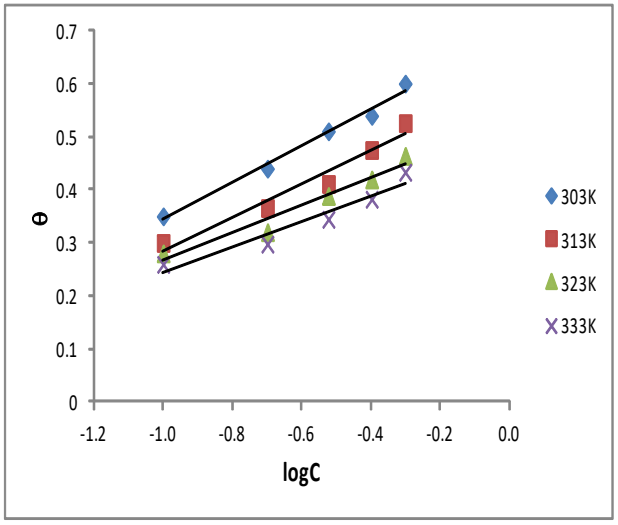

Fig. 12: Temkin isotherm for the adsorption of OPW on aluminium surface at various temperatures.

The free energy of adsorption can be calculated from adsorption constant using the Gibb Helmholtz equation, which is given as (Eddy *et al.,* 2018)

$$\Delta G^0_{ads} = -2.303RTlog(55.5 \times b_{ads}) \quad (17)$$

Free energy change in the range of -20 to -40 kJ/mol are associated with chemical adsorption mechanism but outside this range, physiosorption mechanism dominates. The calculated free energy is recorded in Table 6 and reflects that the adsorption of OPW on aluminum is dominated by physiosorption.

Table 5: Temkin parameters for the adsorption of OPW on aluminium surface at various temperatures

T (K)	Slope	Intercept	A	logb	ΔG^0_{ads} (J/mol)	R^2
303	0.3471	0.6912	3.32	0.1042	-10.72	0.9872
313	0.3147	0.5997	3.66	0.0819	-10.94	0.9548
323	0.2629	0.5284	4.38	0.0603	-11.16	0.9523
333	0.2391	0.4833	4.82	0.0502	-11.44	0.9310

Freundlich adsorption equation is given by equation 18 ((Ngobiri *et al*., 2015)

$$log\theta = logb_{ads} + nlog[C] \quad (18)$$

From the above equation, Freundlich isotherm is applicable when a plot of logθ against log*[C] gives* a straight line with slope and intercept equal to 'n' and $logb_{ads}$ respectively. Freundlich isotherm for the adsorption of OPW on aluminum surface is shown in Fig. 13 while the adsorption parameters calculated from the slopes and intercepts are recorded in Table 6. The results indicated that the adsorption strength (which can be measured by n and b_{ads} values) decreased with increase in temperature indicating that the adsorption of this inhibitor is likely through physiosorption mechanism ((Khadom and Abod, 2016) Theoretically, the adsorption of an inhibitor on the surface of the metal can be regarded as a simple substitution process involving the substitution of x molecule of water by the inhibitor's molecules according to the following equation

$$I_{aq} + xH_2O = I_{ads} + xH_2O \quad (19)$$

where *x* is the size ratio and equals the number of adsorbed water molecules replaced by a single inhibitor molecule. Applying Freundlich model, x can be equated to be equal to 'n' and from the results, values of n decreases with temperature.

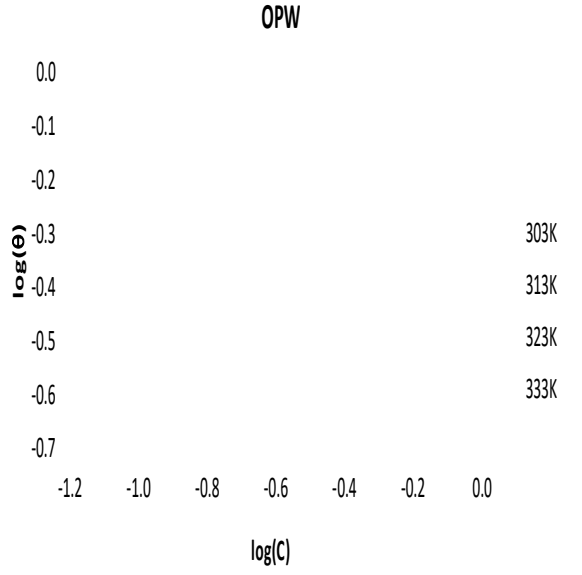

Fig. 13: Freundlich Isotherm for the adsorption of OPW on the surface of Al.

This implies that as the temperature increases, the number of water molecules that is displaced by OPW molecules decreases, hence the adsorption is reduced as the temperature increases. Free energy changes obtained from Freundlich adsorption were also within the range established for physiosorption mechanism (Table 7)

Table 6: Freundlich parameters for the adsorption of OPW on the surface of Al

T (K)	$logb_{ads}$	n	ΔG^0_{ads} (J/mol)	R^2
303	-0.1268	0.33	-9.36	0.995
313	-0.1886	0.34	-9.00	0.9827
323	-0.2479	0.32	-8.66	0.9717
333	-0.2889	0.31	-8.42	0.9631

The El-Awady *et al* kinetic isotherm (equation 20) can provide further insight into the strength of adsorption.,

$$\log\left(\frac{\theta}{1-\theta}\right) = logb' + ylogC \quad (20)$$

where y is the number of inhibitor molecules occupying one active site and 1/y represents the number of active sites on the surface occupied by one molecule of the inhibitor. 'y' is also related to the binding constant, B through $B = b'^{\left(\frac{1}{y}\right)}$. Fig. 14 shows El-Awady *et al* plots for the adsorption of OPM on the surface of Al. Adsorption parameters from the plots are recorded in Table 7

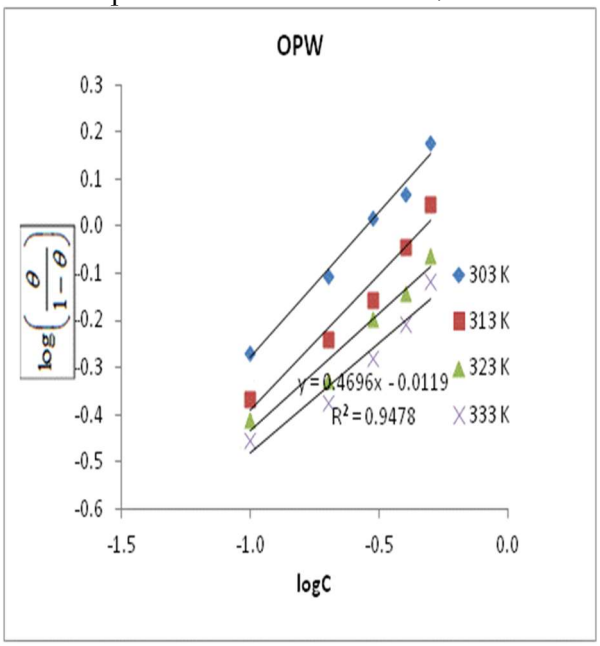

Fig. 14: El awardy et al isotherm for the adsorption of OPW on Al surface

Table 7:Adsorption parameters for the adsorption of OPW on Al surface according to El awardy et al isotherms

T (K)	1/y	B	R^2
303	1.621271	1.618575	0.9881
313	1.734605	1.278415	0.965
323	2.005214	1.076768	0.9618
333	2.129472	0.987213	0.9478

From the slopes of the plots, values of 1/y are observed to be greater than unity indicating the existence of multimolecular layer of adsorption. Also, calculated values of B were found to decrease with temperature which implies that at lower temperature, the adsorption is better and may be attributed to stronger electrical interaction between the double layer existing at the phase boundary and the adsorption molecule. On the other hand, at higher temperature, the interaction between the adsorbing molecules and the metal surface is weak.

Dubinin-Radushkevich isotherm was also used to investigate the mechanism of adsorption of OPW on aluminum surface. The Dubinin-Radushkevich (D-RIM) adsorption isotherm can be expressed according to equation 21 (Noor, 2009),

$$\ln\theta = \ln\theta_s - a\sigma^2 \qquad (21)$$

where θ_{max} is the maximum surface coverage and σ is the polany potential and can be estimated from the following equation,

$$\sigma = RT\ln\left(1 + \frac{1}{C}\right) \qquad (22)$$

Therefore, a plot of lnθ versus σ^2 should give a straight line (as shown in Fig.15) with slope equals to a constant, 'a'. This constant, 'a' can be defined as half the square of the reciprocal of the mean adsorption energy (i.e. a = ½ $(1/E)^2$. E value less than 8 kJ/mol supports the mechanism of physical adsorption but E values greater than 8 kJ/mol are consistent with the mechanism of chemisorption (Papoola, 2019),

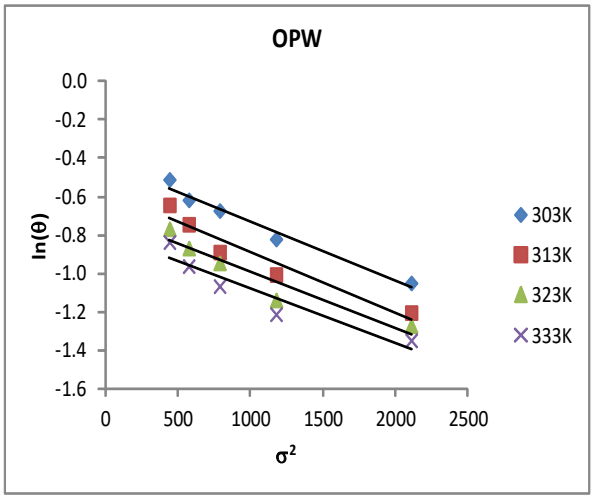

Fig15:Dubinin-Radushkevich isotherm for the adsorption of OPW on Al surface

. From the results obtained (Table 8), the calculated values of the adsorption energy are less than the threshold value of 8 kJ/mol, therefore, the adsorption of OPW onto the surface of aluminium is consistent with the mechanism of charge transfer from charged inhibitor to charged metal surface, which indicates physiosorption mechanism (Wei *et al.,* 2020). Also, calculated free energy changes were less than -20 kJ/mol and confirmed that the adsorption of OPW on aluminum surface progresses through physiosorption mechanism.

Table 8: Dubinin-Radushkevich isotherm adsorption parameters for OPW

T (K)	'a'	Lnx	x	E (J/mol)	R^2
303	0.0003	-0.4194	0.657441	40.82	0.9745
313	0.0003	-0.5741	0.563212	40.82	0.9260
323	00003	-0.7008	0.496188	40.82	0.9111
333	0.0003	-0.7952	0.451491	40.82	0.8882

It is significant to state that the Freundlich and Temkin isotherms did not fit the adsorption of OPW in the presence of the halide ions. However, only Langmuir adsorption isotherm best described joint adsorption of OPW and halides on aluminum surface. The Langmuir adsorption equation takes the form of equation 20 (El Shami *et al*., 2020)

$$log\left(\frac{C}{\theta}\right) = logC - logb_{ads} \qquad (23)$$

The Langmuir isotherm plots indicating the variation of $log(C/\theta)$ versus logC for the adsorption of OPW (at different temperatures) and for joint adsorption of OPW and halide ions on aluminum surface are shown in Fig. 17 while Table

9 presents the Langmuir adsorption parameetrs Interesting results indicated that the adsorption plots in the presence of halide ions approaches different direction (negative slope) as opposed to the adsorption of OPW at different temperatures. This means there is a complete change in mechanism in the presence of the halide ions. According to Eddy and Ita (2011a), when the Langmuir isotherm has a negative slope, the mechanism is likely chemical adsorption. However, such negative slopes were observed for joint adsorption of OPW and halides but calculated values of changes in free energy reflected physical adsorption mechanism because they were negatively less than the threshold value of – 40 kJ/mol. However, Eddy and Ita (2011b) has also deduced that before chemisorption mechanism can be initiated, initial physiosorption process may be necessary at lower temperature but at higher temperature, chemisorption dominates.

Therefore, joint adsorption of OPW and halides proceeded through the mechanism of chemisorption. The Langmuir isotherm also assumes that the slope values should be unity (Anand and Chitra, 2020). This implies that as the slope tends to unity, ideality of the Langmuir isotherm becomes more certain, that is, there is no interaction between the adsorbed species. Slope values for the adsorption of OPW on aluminum surface were low at all temperatures (range = 0.5698 to 0.5835) but higher in the presence of halide ions (range = 0.5873 to 0.9757).

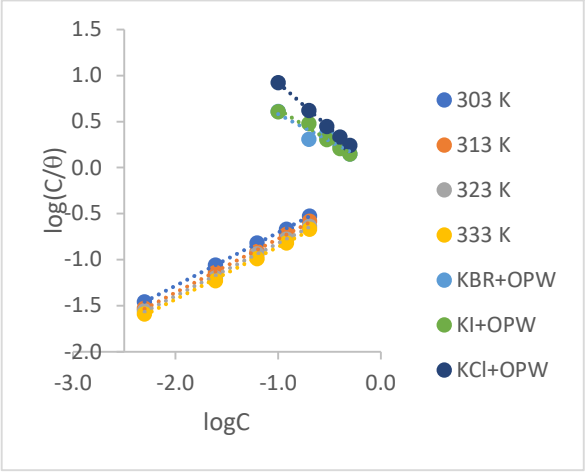

Fig. 17: Langmuir isotherm for the adsorption of OPW and for joint adsorption of OPW and halide ions on aluminum surface

This shows an improvement in the adsorption of the inhibitor through synergistic interaction. Improvement in adsorption was also observed in calculated free energy changes, which were negatively higher in the presence of halide ions (Table 9).

Table 9: Langmuir parameters for the adsorption of OPW and for joint adsorption of OPW and halides on the surface of aluminum.

T (K)	Slope	b_{ads}	ΔG^0_{ads} (kJ/mol)	R^2
303 K(OPW)	0.5768	-0.1268	-9384.02	0.9997
313 K(OPW)	0.5835	-0.1886	-9025.48	0.9988
323K (OPW)	0.5722	-0.2479	-8681.45	0.9983
333K (OPW)	0.5696	-0.2889	-8443.58	0.9978
303 K (OPW+KBR)	-0.5830	-0.0003	-10117.9	0.871
303 K (OPW+KI)	-0.6801	-0.0452	-9857.43	0.9747
303 K(OPW+KCl)	-0.9757	-0.0537	-9808.12	0.9995

3.5 FTIR study

FTIR study is one of the methods that can be used to identify functional groups that are available in the inhibitors. Corrosion inhibition process is an adsorption process that is facilitated by the presence of hetero atoms or suitable functional groups. Table 10 presents frequencies and functional group assignments that are associated with the absorption of IR by OPW. The FTIR spectrum of OPW revealed the present of OH stretch vibrations at 3407, CH stretch vibration at 2929 cm^{-1}, -C≡C- stretch at 2156 cm^{-1}, -C=C- stretch at 1648 cm^{-1}, NO asymmetric stretch at 1543 cm^{-1}, C-C stretch at 1424 cm^{-1}, C-N stretch at 1254 cm^{-1}C-O stretch at 1032 cm^{-1} and CX stretch at 587 cm^{-1}. The spectrum also reveals the presence of hetero atoms and suitable functional groups in OPW waste. Hence OPW possesses require features that support its corrosion inhibition efficiency (Awe *et al*., 2019; Odoemelam *et al*., 2020).

Table 10: Frequencies and intensity of IR absorption by OPW for various assigned functional groups

Frequency (cm^{-1})	Intensity	Functional group
587.34	39.5792	C-X stretch
1031.95	19.3137	C-O stretch
1253.77	39.3884	C-N stretch
1423.51	34.1681	C-C stretch
1543.1	42.9718	N-O asymmetric
1648.23	29.0517	-C=C- stretch
2155.52	74.2258	-C≡C- stretch
2929.0	23.7819	C-H stretch
3407.37	12.2955	OH stretch

4.0 Conclusion

The study reveals that ethanol extract of orange peel contain corrosion inhibitors that combines to exert corrosion inhibitive action on aluminum. The extract is an adsorption inhibitor that that follows physisorption mechanism, However, in the presence of halides ions, the mechanism changes to chemisorption at higher temperatures. Freundlich, Temkin, El Awardy and Dubinin Raduskevich models sufficiently describes the adsorption characteristics of the inhibitor. Although Langmuir adsorption isotherm gave excellent degree of fitness, the non-ideality of the plots indicated that there is some interaction between the adsorbed species. Joint effect of halides and OPW gave better ideality to the Langmuir adsorption model.

5.0 Acknowledgement

I acknowledge with thanks, the contributions of my Ph. D supervisors, Prof. Nnabuk Okon Eddy and Prof. Steven A. Odoemelam, towards the research that yielded this publication.

6.0 References

Agrawal, Y. K., Talati, J. D., Shah, M. D, Desai, M. N & Shah, N. K. (2003). Schiff bases of ethylenediamine as corrosion inhibitors of zinc in sulphuric acid. *Corrosion Science,* 46, pp. 633-651.

Ameh, P. O.& Eddy, N. O. (2018). Theoretical and experimental investigations of the corrosion Inhibition action of *Piliostigma thonningii* extract on mild steel in acidic medium. Communication in Physical Sciences 3, 2, pp. 27-42.

Awe, F. E., Abdulwahab, M. & Otaru, H. A. (2019). Adsorptive studies of the inhibitive properties of ethanolic extracts of *Parinari polyandra* on mild steel in acidic media. Communication in Physical Sciences, 4, 1, 49-57.

Ebenso, E. E., Eddy, N. O. & Odiongenyi, A. O. (2008). Corrosion inhibitive properties and adsorption behaviour of ethanol extract of *Piper guinensis* as a green corrosion inhibitor for mild steel in H_2SO_4. *African Journal of Pure and Applied Chemistry, 4*, 11, pp. 107-115.

Eddy N. O, Ebenso E. E (2010) Corrosion inhibition and adsorption properties of ethanol extract of *Gongronema latifolium* on mild steel in H_2SO_4 *Pigment and Resin Technology* 39(2): 77-83.

Eddy, N. O, Ekwumengbo, PA, Mamza, PAP (2009c) Ethanol extract of *Terminalia catappa* as a green inhibitor for the corrosion of mild steel in H_2SO_4 *Green Chemistry Letters and Review* 2, 4, pp. 223-231

Eddy NO (2010) Theoretical study on some amino acids and their potential activity as corrosion inhibitors for mild steel in HCl. *Molecular Simulation*, 35, 5, pp. 354-363.

Eddy, N. O., Odoemelam, S. A. & Odiongenyi, A. O . (2009) Joint effect of halides and ethanol extract of *Lasianthera Africana* on the inhibition of the corrosion of mild steel in H_2SO_4 *Journal of Applied Electrochemistry*, 39, 6, pp. 849 – 857.

Eddy, N. O, Ibok, U. J., Ameh, P. O., Alobi, N. O. & Sambo, M. M. (2014). Adsorption and quantum chemical studies on the inhibition of the corrosion of aluminum in HCl by *Gloriosa superba* (GS) gum *Chemical Engineering Communications*, 201, 10, pp. 1360-1383

Eddy, N. O, Awe, F. E. & Ebenso, E. E. (2010). Adsorption and inhibitive properties of ethanol extracts of leaves of *Solanum melongenid* for the corrosion of mild steel in 01M HCl *International Journal of Electrochemical Science*, 5, pp. 1996-2011.

Eddy, N. O. & Awe, F. E. (2018). Experimental and quantum chemical studies on ethanol extract of *Phyllanthus amarus* (EEPA) as a green corrosion inhibitor for aluminium in 1 M HCl. *Portugaliae Electrochimica Acta*, 36, 4, pp. 231-247

Eddy, N. O. & Mamza,, P. A. P. (2009). Inhibitive and adsorption properties of ethanol extract of seeds and leaves of *Azadirachta indica Portugaliae Electrochimica* Acta, 27, 2, pp. 20-28.

Eddy, N. O. & Odiongenyi, A. O. (2010). *Corrosion inhibition and adsorption properties of ethanol extract of Heinsia crinata on mild steel in H_2SO_4 Pigment and Resin Technology*, 38(, 5, pp. 288-295.

Eddy, N. O. & Odoemelam, S. A. (2009). Inhibition of the corrosion of mild steel in H_2SO_4 by ethanol extract of *Aloe vera. Resin and Pigment Technology*, 38, 2, pp. 111-115.

Eddy, N. O. (2009). Ethanol Extract of *Phyllanthus Amarus* as a Green Inhibitor for the Corrosion of, ild Steel in H_2SO_4- *Portugaliae Electrochimica Acta*, 27, 5, pp. 579-589.

Eddy, N. O. and Ita, B. I. (2011). Theoretical and experimental studies on the inhibition potentials of aromatic oxaldehydes for the corrosion of mild steel in 0.1 M HCl. *Journal of Molecular Modeling* 17, pp. 633-647

Eddy, N. O., Ameh, P. O., Gimba, E. E. & Ebenso, E. E. (2011). GCMS studies on *Anogessus leocarpus* gum and their corrosion inhibition potential for mild steel in 0.1 M HCl. *International Journal of Electrochemical Sciences*, 6, pp. 5815-5829.

Eddy, N. O., Ita, B. I., Dodo, S. N., Paul E. D. (2011) Inhibitive and adsorption properties of ethanol extract of *Hibiscus sabdariffa* calyx for the corrosion of mild steel in 01 M HCl *Green Chemistry Letters and Review*, 5, 1, pp. 43-53

Eddy, N. O., Ita, B. I., Dodo, S. N. & Paul, E. D. (2012). Inhibitive and adsorption properties of ethanol extract of Hibiscus *sabdariffa calyx* for the corrosion of mild steel in 0.1 M HCl. Green Corrosion Letters and Review 5, 1, pp. 43-53.

Eddy, N. O., Momoh-Yahaya, H. & Oguzie, E. E. (2015) Theoretical and experimental studies on the corrosion inhibition potentials of some purines for aluminium in 01 M HCl *Journal of Advanced Research*, 6, pp.203-216.

Eddy, N. O., Odiongenyi, A. O., Ameh, P. O, &Ebenso E. E. (2012) Corrosion inhibition potential of *Daniella oliverri* gum exudate for mild steel in acidic medium *International Journal of Electrochemical Sciences*, 7, 7425-7439

Eddy, N. O., Odoemelam, S. A., Ibiam, E. (2010). Ethanol extract of *Occimium gratissimum* as a green corrosion inhibitor for mild steel in H_2SO_4 *Green Chemistry Letters and Review*, 3, 3, pp. 165-172

Eddy, N. O., Odoemelam, S. A. & Ama, I. N. (2010). Ethanol extract of *Occimum gratissimum* as a green corrosion inhibitor for the corrosion of mild steel in H_2SO_4. Green Chemistry Letters and Review 3,3, pp. 165-172.

Eddy, N. O., Odoemelam, S. A. & Odiongenyi, A. O. (2009) Inhibitive, adsorption and synergistic studies on ethanol extract of *Gnetum africana* as green corrosion inhibitor for mild steel in H_2SO_4 Green *Chemistry Letters & Review*, 2, 2, pp. 111-119.

Eddy, N. O., Odoemelam, S. A. & Odiongenyi, A. O. (2009). Ethanol extract of Musa species peel as a green corrosion inhibitor for mild steel: Kinetics, adsorption and thermodynamic considerations. Electronic Journal of Environmental, Agricultural and Food Chemistry, 8, 4,

Eddy, N. O. & Ita, B. I. (2011). Experimental and theoretical studies on the inhibition potentials of some derivatives of cyclopenta-1,3-diene. *International Journal of Quantum Chemistry* 111, 14, pp. 3456-3473.

Ella, E. D. & Rodrigues, P., R. P. (2019). Aqueous agro-industrial waste as corrosion inhibitor for stainless steel AISI 304 in acidic media. Materials Research 22, 5, https://dx.doi.org/10.1590/1980-5373-MR-2018-0695

Farag, A. A., Ismail, A. S. & Migahed, M. A. (2018). Environmental-friendly shrimp waste protein corrosion inhibitor for carbon steel in 1 M HCl solution. Egyptian Journal of Petroleum, 27, 4, pp. 1187-1194.

Ismail, M., Abdulrahman, A. S. & Hussain, M. S. (2011). Solid waste as environmental benign corrosion inhibitors in acid medium. International Journal of Engineering and Technology, 3, 2, pp. 1742-1748.

Jovancicervic, V., Ramachadran, S. & Prince, P. (1999). Inhibition of carbon (IV) oxide corrosion of mild steel by imidazoline and their precursors. *National Agency for Corrosion Engineering Journal, .* 55, 5, pp. 449-453.

Khadom, A. A. & Abod, B. M. (2016). Mathematical model for galvanic corrosion of steel-copper couple in petroleum waste water in presence of friendly corrosion inhibitor. *Journal of Applied Research and Technology*, 15, pp. 14-20.

Mishurov, V. I., Shubina, E. N., Klushin, V. A., Chizhikova, A. A., Kashparova, V. P. & Berezhnaya, A. G. (2019). Biomass conversion products as steel corrosion inhibitors. Applied Electrochemistry and Metal Corrosion Protection, 92, pp. 620-624.

Ngobiri, N. C., Oguzie, E. E., Li, Y., Liu, L., Oforka, N. C. & Akaranta, O. (2015). Eco-friendly corrosion inhibition of pipeline steel using *Brassica oleracea. International Journal of Corrosion*, 2015, Article ID 404139, 9 pages http://dx.doi.org/10.1155/2015/404139

Noor, E. A. (2009). Potential of aqueous extract of Hibiscus sabdariffa leaves for inhibiting the corrosion of aluminum in alkaline solutions. *Journal of Applied Electrochemistry*, 39, pp.1465-1475

Ogoko, E. C., Odoemelam, S. A., Ita, B. I. & Eddy, N. O. (2009). Adsorption and inhibitive properties of clarithromycin for the corrosion of Zn in 0.01 to 0.05 M H_2SO_4. *Portugaliae Electrochimica. Acta,* 27, 6, pp. 713-724.

Papoola, L. T. (2019). Organic green corrosion inhibitors (OGCIs): a critical review. Corrosion Review, 37, 2. I: https://doi.org/10.1515/corrrev-2018-0058

Stango, A. X. & Vijayalakshmi, U. (2018) Studies on corrosion inhibitory effect and adsorption behavior of waste materials on mild steel in acidic medium. *Journal of Asian Ceramic Societies*, 6, 1, pp. 20-29,

Wei, W., Liu, Z., Liang, C., Han, G., Han, J. & Zhang, S. (2020). Synthesis, charactization and corrosion inhibition behaviour of 2-aminoflurene bis-Schiff bases in circulating cooling water. *Royal Society of Chemistry Advances*, 10, pp. 17816-17828.

Ye, Y., Yang, D. & Chen, H. (2019). A green and effective corrosion inhibitor of functionalized carbon dots. *Journal of Materials Science and Technology*, 35, 10, pp. 2243-2253. Yurt, A., Balabam, A., Kandemer, S. U., Bereket, G. & Erk, B. (2004). Investigation some Schiff bases as HCl corrosion inhibitors for carbon steel. *Material Chemistry and Physics,* 85, p. 420 -426.